

Effects of energy loss on interaction dynamics of energetic electrons with plasmas

C. K. Li and R. D. Petrasso

Plasma Science and Fusion Center, Massachusetts Institute of Technology, Cambridge, Massachusetts 02139, USA

(Received 5 May 2009; published 12 October 2009)

An analytic model is developed for energetic electrons interacting with plasmas. This model rigorously treats the effects of energy loss upon Coulomb interactions and reveals several important features, including the coupling of scattering and energy loss—which previous calculations had erroneously treated as independent in cases where an electron lost a significant amount (or all) of its energy. The unique transparency and generality of these calculations allows for straightforward applications when quantitatively evaluating the energy deposition of energetic electrons in various plasmas, including those in inertial confinement fusion.

DOI: [10.1103/PhysRevE.80.047402](https://doi.org/10.1103/PhysRevE.80.047402)

PACS number(s): 52.40.Mj, 52.50.Gj, 52.20.Fs

The interaction of energetic electrons with plasmas is a fundamental problem with important implications for both basic physics and practical applications [1–6]. This interaction involves electron energy loss and scattering which leads to electron energy deposition and trajectory bending in plasmas. In the context of a single electron interacting with plasmas, such scatterings alter electron distributions, resulting in modifications of the energy deposition structure [7–9].

In addressing electron interactions with plasmas, the convention is that while they scatter off the plasma ions, energetic electrons lose their kinetic energy to the plasma electrons. The two physics processes (i.e., energy loss and scattering) have been treated independently and combined in a simple way. For example, the mean square of the total deflection angle can be calculated simply by averaging over the solid angle

$$\langle \theta^2 \rangle = \frac{N_c \int \theta^2 \left(\frac{d\sigma}{d\Omega} \right) d\Omega}{\int \left(\frac{d\sigma}{d\Omega} \right) d\Omega}, \quad (1)$$

where N_c is the number of the collisions (which is a function of the electron energy loss and can be independently evaluated) [10]. The treatment of the scattering is exclusively manifested by the integral $\int \theta^2 (d\sigma/d\Omega) d\Omega$. It has been demonstrated that this approach is justified and is accurate for energetic electrons interacting with “thin” targets (e.g. thin solid foils) [11] since an electron suffers only a relatively small number of collisions and the energy loss of each individual collision is very small compared to its total kinetic energy (due to the nature of small angle dominant Coulomb interactions.) Because of this, the energy dependence in the scattering cross sections can be essentially overlooked.

However, such a thin approximation is unjustified and inaccurate when it is applied in the case where an electron loses a significant amount or all of its energy (e.g., during plasma heating) and suffers a very large number (over $\sim 10^6$) collisions, or when an electron interacts with hydrogenic plasmas ($Z=1$, for which the $e-e$ scattering could be comparable with the e -ion scattering). This is explained in Fig. 1 where e -ion (Rutherford) and $e-e$ (Møller) scattering cross sections are plotted as a function of the energy loss $[\Delta E = (E_0 - E)/E_0]$ for 1 MeV electrons in hydrogenic plasmas.

When ΔE changes from beginning to the end ($0 \rightarrow 100\%$ of the energy loss), these cross sections increase about 3 orders of magnitudes, indicating that the effects of energy loss on scattering cannot be ignored in these cases, and that a rigorous approach to the coupling of the energy loss to scattering is necessary. In this Brief Report, we demonstrate the importance of the effects of energy loss upon scatterings in the interaction regime described above using fundamental principles [7–9]. This model naturally links scattering and energy loss, and reveals several of the resulting new and important effects.

In our approach [7–9], an integrodifferential diffusion equation is solved to rigorously determine the angular and spatial distributions of the scattered electrons:

$$\frac{\partial f}{\partial s} + \mathbf{v} \cdot \nabla f = n_i \int [f(\mathbf{x}, \mathbf{v}', s) - f(\mathbf{x}, \mathbf{v}, s)] \sigma(|\mathbf{v} - \mathbf{v}'|) d\mathbf{v}', \quad (2)$$

where $f(\mathbf{x}, \mathbf{v}, s)$ is the electron distribution function; n_i the number density of fully ionized, uniform time invariant background plasma ions of charge Z ; \mathbf{x} the position where scattering occurs; s is the arc length traveled by the electron; $\sigma = \sigma_{ei} + Z\sigma_{ee}$ the total scattering cross section with σ_{ei} the Rutherford e -ion cross section [12], and σ_{ee} the Møller $e-e$

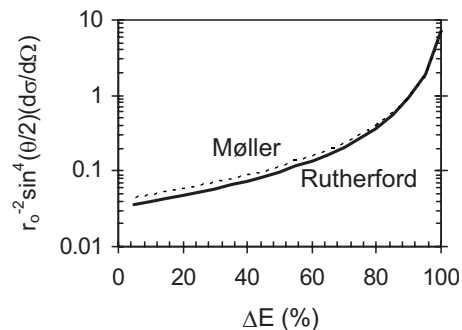


FIG. 1. The normalized Rutherford cross section (e -ion scattering) and Møller cross section ($e-e$ scattering) are plotted as a function of the fraction of the energy loss for 1 MeV electrons. Both cross sections show the significant increase in scattering as an electron loses its energy. For vertical axis, $r_0 = e^2/m_0c^2$ is the classical electron radius.

cross section [13]. The equation is solved with cylindrical coordinates with the assumption that the scattering is azimuthally symmetric. Specifically, the angular distribution is [7–9]

$$f(\theta, E) = \frac{1}{4\pi} \sum_{\ell=0}^{\infty} (2\ell+1) P_{\ell}(\cos \theta) \times \exp\left(-\int_{E_0}^E \kappa_{\ell}(E') \left(\frac{dE'}{ds}\right)^{-1} dE'\right), \quad (3)$$

where $P_{\ell}(\cos \theta)$ is the Legendre polynomial. In this solution, the energy loss is manifested by the plasma stopping power [14,15]

$$\frac{dE}{ds} = \frac{-2\pi r_0^2 m_0 c^2 n_i Z}{\beta^2} \left[\ln\left(\frac{\lambda_D \sqrt{\gamma-1}}{\sqrt{2}\lambda_C}\right)^2 + 1 + \frac{1}{8}\left(\frac{\gamma-1}{\gamma}\right)^2 - \left(\frac{2\gamma-1}{\gamma^2}\right) \ln 2 + \ln\left(\frac{1.123\beta}{\sqrt{2kT_e/m_0c^2}}\right)^2 \right], \quad (4)$$

where $\beta=v/c$ and $\gamma=(1-\beta^2)^{-1/2}$, $r_0=e^2/m_0c^2$ is the classical electron radius, $\lambda_C=\hbar/m_0c$ is electron Compton wavelength, and $\lambda_D=(kT/4\pi n_e e)^{1/2}$ is Debye length. Note that Eq. (4) is valid when $\beta \gg \alpha (=1/137)$, however, its classical counterpart would be accurate enough when $\beta < \alpha$ for which the plasma Debye length is shorter than the electron deBroglie length, such as in the case of low-energy electron preheating inertial confinement fusion (ICF) targets. The effects of scattering are characterized by the ‘‘macro’’ transport cross sections

$$\kappa_{\ell}(E) = n_i \int \left(\frac{d\sigma}{d\Omega}\right) [1 - P_{\ell}(\cos \theta)] d\Omega, \quad (5)$$

where the Legendre polynomial converges rapidly for the large angles. The dominant terms are $\ell=1$

$$\kappa_1(E) = 4\pi n_i \left(\frac{r_0}{\gamma\beta^2}\right)^2 \left[Z^2 \ln \Lambda^{ei} + \frac{4(\gamma+1)^2}{(2^{\sqrt{(\gamma+1)/2})^4} Z \ln \Lambda^{ee}} \right], \quad (6)$$

which is related to the slowing down cross section and characterizes the loss of directed velocity (momentum) in the scattering [4]; and $\ell=2$

$$\kappa_2(E) = 12\pi n_i \left(\frac{r_0}{\gamma\beta^2}\right)^2 \left[Z^2 \left(\ln \Lambda^{ei} - \frac{1}{2} \right) + \frac{4(\gamma+1)^2}{(2^{\sqrt{(\gamma+1)/2})^4} Z \left(\ln \Lambda^{ee} - \frac{1}{2} \right)} \right], \quad (7)$$

which is related to the deflection cross section and represents the mean-square increment in the transverse electron velocity during the scattering process [4]. It should be noted that such simple analytic versions of transport coefficients [Eqs. (6) and (7)] are only valid for $\gamma < \sim 10$ [7–9], because to have a small angle-interaction dominant Rutherford-like Møller cross section, several approximations have been made (e.g., the effects of large-angle scattering, as well as higher-order terms in the expansions have been neglected). Equation (8)

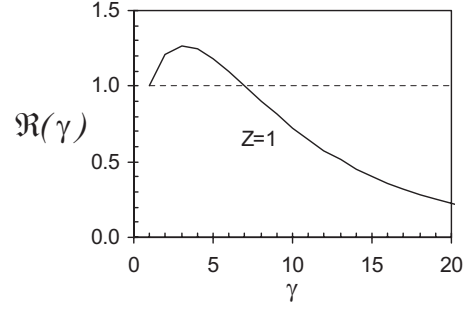


FIG. 2. The ratio of e - e scattering cross section to e -ion scattering cross section is plotted as a function of γ .

gives the ratio of such a simplified Møller cross section [7–9] to Rutherford cross section

$$\mathfrak{R}(\gamma) = Z \left(\frac{d\sigma}{d\Omega}\right)^{ee} / \left(\frac{d\sigma}{d\Omega}\right)^{ei} \approx \frac{4(\gamma+1)^2}{(2^{\sqrt{(\gamma+1)/2})^4} Z}. \quad (8)$$

This ratio is plotted in Fig. 2 for hydrogenic plasmas ($Z=1$), $(d\sigma/d\Omega)^{ee}$ is slightly larger ($\sim 20\%$) than $(d\sigma/d\Omega)^{ei}$ for $\gamma < 7$ (consistent with Fig. 1), while significantly smaller for $\gamma > 10$. Figure 2 also shows that for a nonrelativistic case ($\gamma=1$), one has $(d\sigma/d\Omega)^{ee} \equiv (d\sigma/d\Omega)^{ei}$ [12]. This clearly indicates that directly applying a nonrelativistic result to the cases of relativistic electron-plasmas interactions, such as fast-ignition ICF [16], results in inaccuracy.

Mutual couplings between energy loss and scatterings are explicitly reflected by the following integrand from Eq. (3),

$$\int_{E_0}^E \kappa_{\ell}(E') \left(\frac{dE'}{ds}\right)^{-1} dE'. \quad (9)$$

The integration is a function of electron residual energy (E). Because there is no restriction on electron energy loss, Eq. (9) is valid in the case of an arbitrary amount of even total energy loss. How the thin approximation decouples the effects of energy loss and scattering is discussed below: by assuming the energy dependence of κ is weak, so the scattering effects can be approximately factored out from the integration in Eq. (9).

$$\int_{E_0}^E \kappa_{\ell}(E') \left(\frac{dE'}{ds}\right)^{-1} dE' \approx \kappa_{\ell}(E) \int_{E_0}^E \left(\frac{dE'}{ds}\right)^{-1} dE' = \kappa_{\ell}(E) S(E) \approx \kappa_{\ell}(E) t. \quad (10)$$

Where t is the thickness of the plasma and when it is thin, we find that $t \approx S(E) = \int_0^S ds' = \int_{E_0}^E (dE'/ds) dE'$. The linkage of energy loss to scattering is implied by the relationship between the distance that an electron transverses and energy loss, since the farther an electron transverses, the more energy it loses and the more scatterings it suffers. The approximation in Eq. (10) makes sense when ΔE is very small such that $d\sigma/d\Omega$ in Eq. (5) can be treated as independent of the energy. As a consequence, the calculation with a scattering parameter κ_{ℓ} being factored out of the integration in Eq. (10) is thus justified, and indicates that scattering and energy loss have been treated separately. However, this approximation, as discussed above and shown in Fig. 1, is unjustified in the

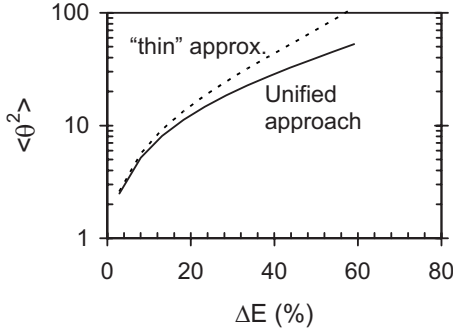


FIG. 3. Mean-square deflection angle $\langle \theta^2 \rangle$ calculated from the unified approach, which has taken into account the effect of energy loss on electron scattering (solid line), and is compared with the conventional thin approximation (dashed line).

cases of total or even significant energy losses of energetic electrons in the plasmas which this paper is focused on.

To further illustrate the effects of energy loss on scattering, we calculate the mean-square deflection angle $\langle \theta^2 \rangle$ from Eq. (9). For the sake of simplicity, the Fokker-Planck approximation is used [by expanding the Legendre polynomial to the power of θ^2 and keeping only the first two terms [17], i.e., $P_\ell(\cos \theta) \approx 1 - 0.25\ell(\ell+1)\theta^2$]. Using Eq. (3) and conducting the integration, the first-order approximation in terms of $\int_0^E \kappa_\ell(s') ds'$ for an exponential function results in

$$\int_{E_0}^E \kappa_\ell(s') \left(\frac{dE'}{ds} \right)^{-1} dE' \approx \frac{1}{4} \ell(\ell+1) \langle \theta^2 \rangle_{Av}. \quad (11)$$

The $\langle \theta^2 \rangle$ is now ready to be evaluated based on the dominant contributions from $\ell=1$ and $\ell=2$

$$\langle \theta^2 \rangle \approx \sqrt{\langle \theta^2 \rangle_{\ell=1}^2 + \langle \theta^2 \rangle_{\ell=2}^2}. \quad (12)$$

where

$$\langle \theta^2 \rangle_{\ell=1} = 2 \int_{E_0}^E \kappa_1(E') \left(\frac{dE'}{ds} \right)^{-1} dE'. \quad (13)$$

and

$$\langle \theta^2 \rangle_{\ell=2} = \frac{2}{3} \int_{E_0}^E \kappa_2(E') \left(\frac{dE'}{ds} \right)^{-1} dE'. \quad (14)$$

Figure 3 compares the $\langle \theta^2 \rangle$ calculated from Eq. (12) and Eq. (1). As shown, a significant difference occurs when electrons have lost more energy.

Another important result from this unified model is that the phenomenological *ad hoc* cutoffs (required to prevent mathematical divergence in the two-body Coulomb interactions) have been effectively removed or significantly reduced because of the inclusion of energy loss in the electron scatterings. The choosing of a suitable model for plasma screening and performing this phenomenological cutoff are usually nontrivial undertakings. The *ad hoc* cutoffs directly reflect the approximations made in the theoretical formulations. Depending on the different plasma densities and temperatures, for example, the screening distances can be determined by either Debye length, Thomas-Fermi screening length (λ_{TF}

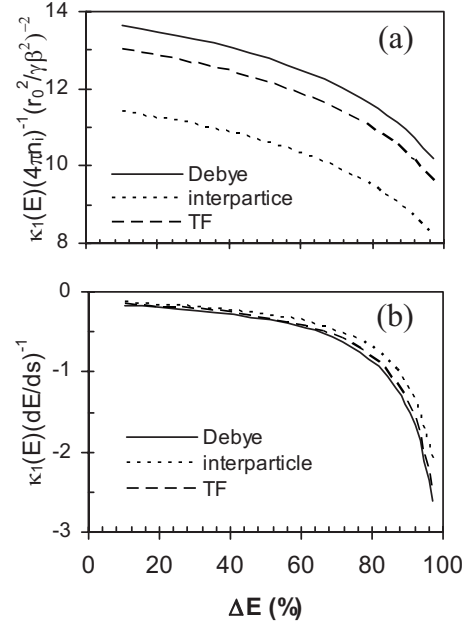


FIG. 4. Using different screening models (Debye, Thomas-Fermi, and interparticle distance), the normalized κ_1 are plotted as a function of the electron energy in DT plasma ($\rho=300$ g/cm³ and $T_e=5$ keV) (a). As is shown, the difference indicates the importance of properly choosing the screening parameters if the elastic scatterings are treated independently. However, as is seen in (b), these differences are dramatically reduced when we take the approach that energy loss and scattering are coupled.

$=0.885a_0Z^{-1/3}$, where $a_0 \equiv \hbar^2/me^2$ is the Bohr radius), or mean interparticle distance ($\lambda = \lambda_{Int} = n^{-1/3}$). The Debye length from an exponential screened Coulomb potential [10],

$$\phi(r) = \phi_0 e^{-r/\lambda_D}, \quad (15)$$

describes the shielding distance at which the potential falls to its e folding from its maximum. The Thomas-Fermi screening length, (a result derived originally from nuclear screening, with corrections for the effects of plasma temperature and density) is a reasonable approximation for ideal gas. Also, the mean interparticle distance is an approximation for dense plasmas when the Debye length is even smaller than the mean interparticle distance.

Such a model constraint is largely relaxed due to the effective cancellation embedded in Eq. (9). For example, the electron deflection is a function of product of energy loss (dE/ds) with scatterings (κ_1),

$$\kappa_1(E) \left(\frac{dE}{ds} \right)^{-1} \propto \frac{\ln \Lambda^{ei} + \frac{4(\gamma+1)^2}{(2\sqrt{\gamma+1}/2)^4} \ln \Lambda^{ee}}{\ln \Lambda}. \quad (16)$$

The effective cancellation of the Coulomb logarithms [7] in the numerator and denominator of Eq. (16) significantly reduces the sensitivity of the selection of plasma screening models. The physics behind such a cancellation can be understood as the deflection occurring simultaneously during the slowing down and scattering-off of the energetic electrons in the encountering plasma mediums. This is illustrated

in Fig. 4, where the normalized transport cross sections $[\kappa_1(E)(4\pi n_i)^{-1}(r_0^2/\gamma\beta^2)^{-2}]$ are plotted as a function of the energy loss [Fig. 4(a)], and differences exist for different models. As shown in Fig. 4(b) where $\kappa_1(E)(dE/ds)^{-1}$ is plotted as a function of energy loss, negligible differences make the effects of different screening models insignificant.

In summary, we have used an analytical model to rigorously examine the effects of energy loss upon the Coulomb interactions, which results in revealing of several new and important findings never before realized, including the coupling of scattering and energy loss. The unique transparency

and generality of these calculations allows for straightforward applications in the cases of partial to even total energy loss of energetic electrons: for example, the quantitative evaluation of the energy deposition of energetic electrons in various plasmas, including those of inertial confinement fusion.

This work was supported in part by U.S. Department of Energy Contract (Grants No. DE-FG52-07NA28059 and No. DE-FG52-06N826203), LLE (Grant No. 414090-G), the Fusion Science Center at University of Rochester (Grant No. 412761-G).

-
- [1] G. Moliere, Z. Naturforsch. B **3a**, 78 (1947).
 [2] H. A. Bethe, Phys. Rev. **89**, 1256 (1953).
 [3] L. Spitzer, *Physics of Fully Ionized Gases* (Interscience, New York, 1962).
 [4] B. Trubnikov, *Review of Plasma Physics* (Consultants Bureau, New York, 1965).
 [5] C. K. Li and R. D. Petrasso, Phys. Rev. Lett. **70**, 3059 (1993).
 [6] C. K. Li and R. D. Petrasso, Phys. Rev. Lett. **70**, 3063 (1993).
 [7] C. K. Li and R. D. Petrasso, Phys. Rev. E **70**, 067401 (2004).
 [8] C. K. Li and R. D. Petrasso, Phys. Rev. E **73**, 016402 (2006).
 [9] C. K. Li and R. D. Petrasso, Phys. Plasmas **13**, 056314 (2006).
 [10] J. D. Jackson, *Classical Electrodynamics* (Wiley, New York, 1975).
 [11] P. C. Hemmer *et al.*, Phys. Rev. **168**, 294 (1968).
 [12] R. D. Evans, *The Atomic Nucleus* (McGraw-Hill, New York, 1955).
 [13] C. Møller, Ann. Phys. **14**, 531 (1932).
 [14] For the energy loss obtained in Refs. [7–9] we have used the classical version of the maximum impact parameter for *ad hoc* cutoff, which may have resulted in slightly overestimated linear energy loss. In the Brief Report, we have corrected this inaccuracy (see Eq. (4)) by including quantum effects.
 [15] A. A. Solodov and R. Betti, Phys. Plasmas **15**, 042707 (2008).
 [16] M. Tabak *et al.*, Phys. Plasmas **1**, 1626 (1994).
 [17] H. W. Lewis, Phys. Rev. **78**, 526 (1950).